

Supplementary Material

Design of a multi-tubular catalytic reactor assisted by CFD based on free-convection heat-management for decentralised synthetic methane production

Andreina Alarcón^{1,2}, Raquel Busqué³, Teresa Andreu^{1,2}, Jordi Guilera^{1,2*}

¹ Catalonia Institute for Energy Research (IREC), Jardins de les Dones de Negre 1, 08930 Sant Adrià de Besòs, Spain

² Facultat de Química, Universitat de Barcelona, Martí i Franquès, 1, Barcelona 08028, Spain

³ Eurecat, Centre Tecnològic de Catalunya, Product Innovation & Multiphysics Simulation Unit, Universitat Autònoma, 23, 08290 Cerdanyola del Vallès, Spain

corresponding author: jguilera@irec.cat

Preliminary simulation results

The first set of CFD simulations were conducted on a simple two-reactive channel at two extreme air velocities (0 m/s (natural convection) and 5m/s (forced convection)) to identify the free-convection heat-management strategy for a scalable multi-tubular reactor design. For this simple reactor geometry, the reactive channels were separated by a total length of 25 mm under a lineal-shaped distribution. A $T_{inlet}=230$ °C, $P=5$ atm and $V_{inlet}=0.8$ m/s were used as the reaction conditions. These selected values were the same for all the simulations performed in this simulation-based study. Figure S1 shows the temperature profiles of the two-reactive channel. As it can be seen, a quasi-adiabatic temperature profile ($T=639-530$ °C) in the two-reactive channel was identified at the natural convection condition (without air velocity)(Figure S1a), while a non-isothermal temperature profile ($T=555-167$ °C) was identified at forced convection velocity of 5 m/s (Figure S1b). The high temperatures (639 °C) achieved at 0 m/s along the reactive channel allowed to confirm the need for the implementation of air circulation in the first section of the reactor. At 5 m/s, an interesting temperature behaviour was observed over the two-reactive channel reactor. On the one hand, the implementation of high air velocities was found to be positive to limit the hot spot formation in the first reactor section. The maximum temperature was 555 °C, much lower in comparison to 0 m/s, but out of the selected operative range (230-500°C). This maximum temperature values can be associated with the selected reactive channel separation. A not optimal length between the reactive channels can be negative as a high lateral thermal interaction can be achieved. On the other hand, the implementation of a high air velocity was found to be negative to achieve the optimal temperatures in the last reactor section. A low temperature of 167 °C was identified. An inadequate temperature reaction in this reactor zone can lead to kinetic problems [34,36]. Therefore, in view of this ineffective temperatures, the implementation of an insulation zone to guarantee a suitable temperature at reactor outlet is needed. According to these preliminary findings, a strategy to achieve an easy and feasible multi-tubular reactor operation based on free-convection, two main zones were defined along the height of the reactor. Particularly, it was proposed that in first section of the reactor geometry, the reactive channels should be exposed to ambient air to achieve a maximum temperature at the desired range ($T_{max}<500$ °C), while an insulation material should be only implemented in the last section of the reactor to avoid heat loss to the environment and achieve minimum temperature at the desired range ($T_{max}>230$ °C).

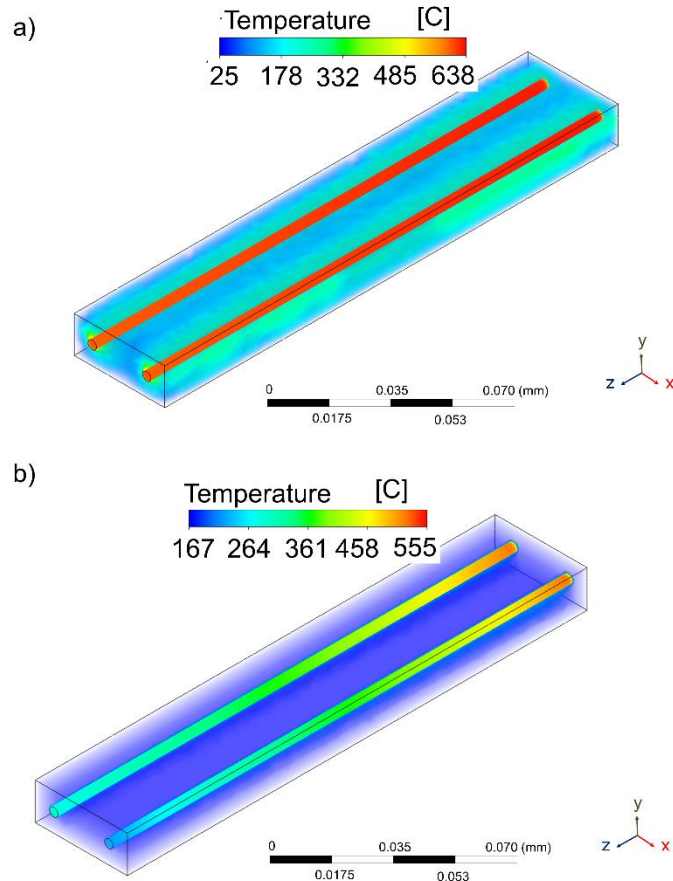


Figure S1. Temperature profile of the multi-tubular fixed-bed reactor configured by two-reactive channel at a) 0m/s and b) 5m/s.

As part of the CFD modelling, the pressure drop along the catalytic bed was additionally estimated to confirm a reliable performance of the scaled-up multi-tubular fixed bed reactor. The Ergun pressure drop correlation was used to represent a gas-solid porous media with an effective heat/mass transfer along of each mm-sized reactive channel. At the selected fractional void volume of 0.74 and 0.40 for the catalytic bed, the theoretical pressure drop was 0.01 and 0.24 bar, respectively. Compared to experimental data, Knobloch et al. [44] in similar systems achieved a pressure drop of 0.1-0.4 bar·m, which represents 0.063 bar, as a result of the height of the bed. Therefore, it can be concluded that the developed numerical approach was accurate enough to calculate catalytic bed to air heat transfer coefficients and thus effectively applicable to investigate the effect of the air flow on the reactor performance in the considered range (0-5 m/s).

Additional Figures

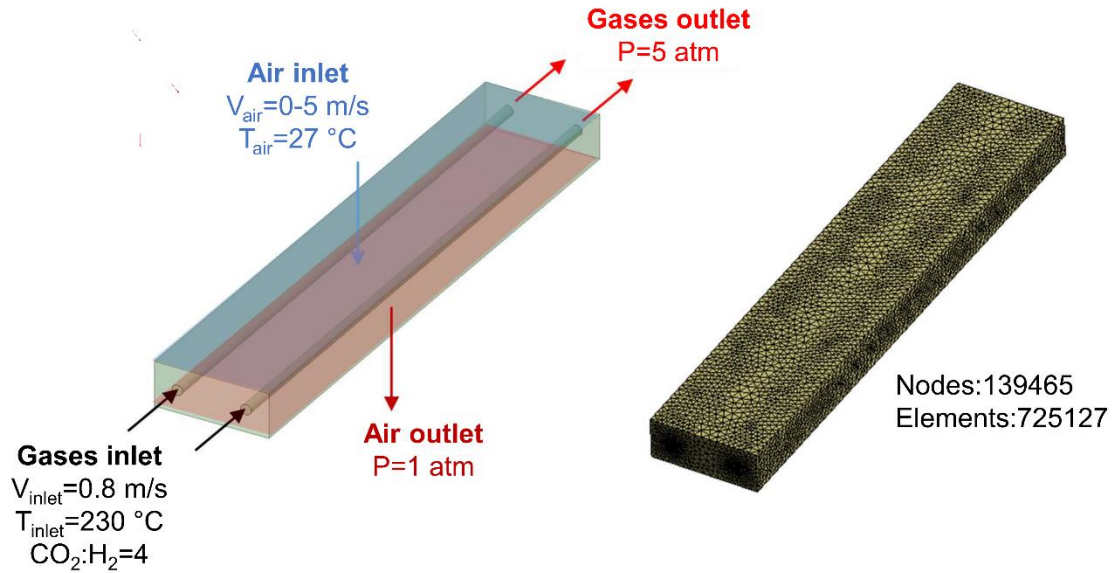


Figure S2. Geometry, boundary conditions and mesh of the multi-tubular fixed bed reactor design. Specification reactor design: Number of reactive channels=2; Geometry configuration=Lineal-shaped distribution; Reactive channel distance separation=25 mm; Free-reactive zone=250 mm

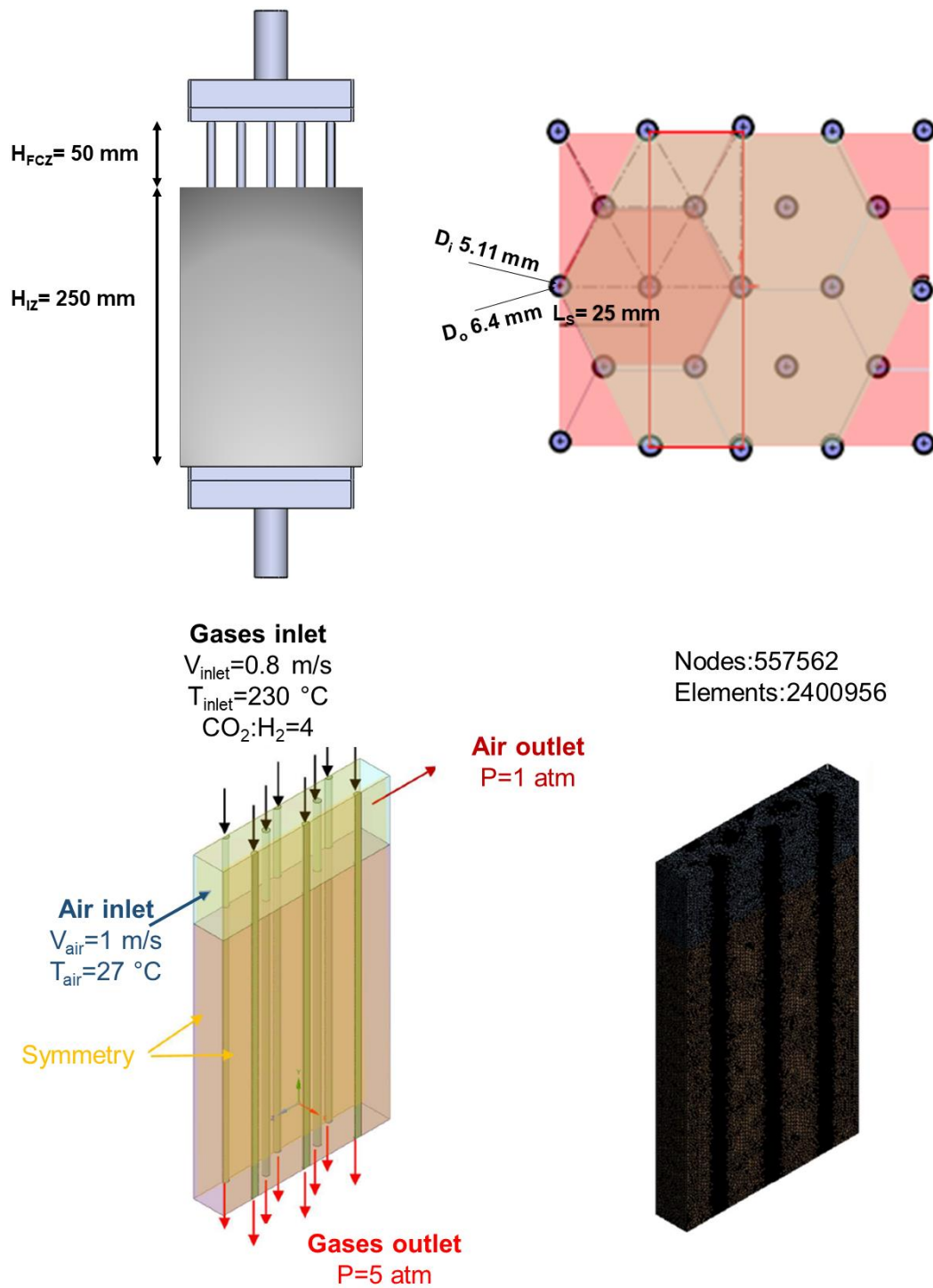


Figure S3. Geometry, boundary conditions and mesh of the multi-tubular fixed bed reactor design. Specification reactor design: Number of reactive channels=19; Geometry configuration=hexagonal-shaped distribution; Reactive channel distance separation=25 mm; Free-reactive zone=50 mm; Insulation active zone=200 mm.

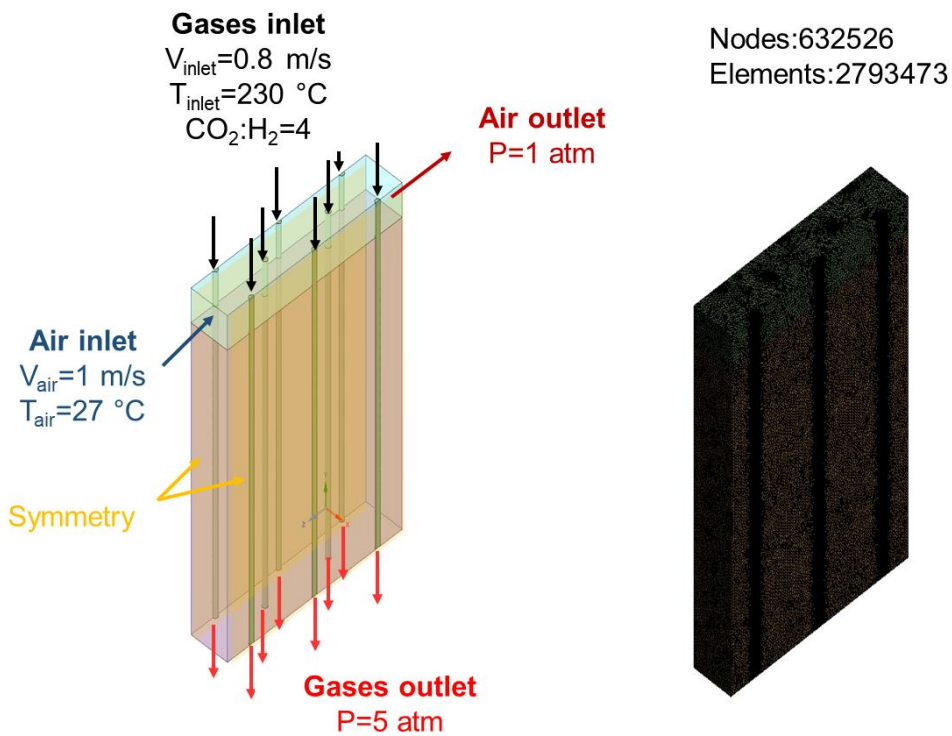
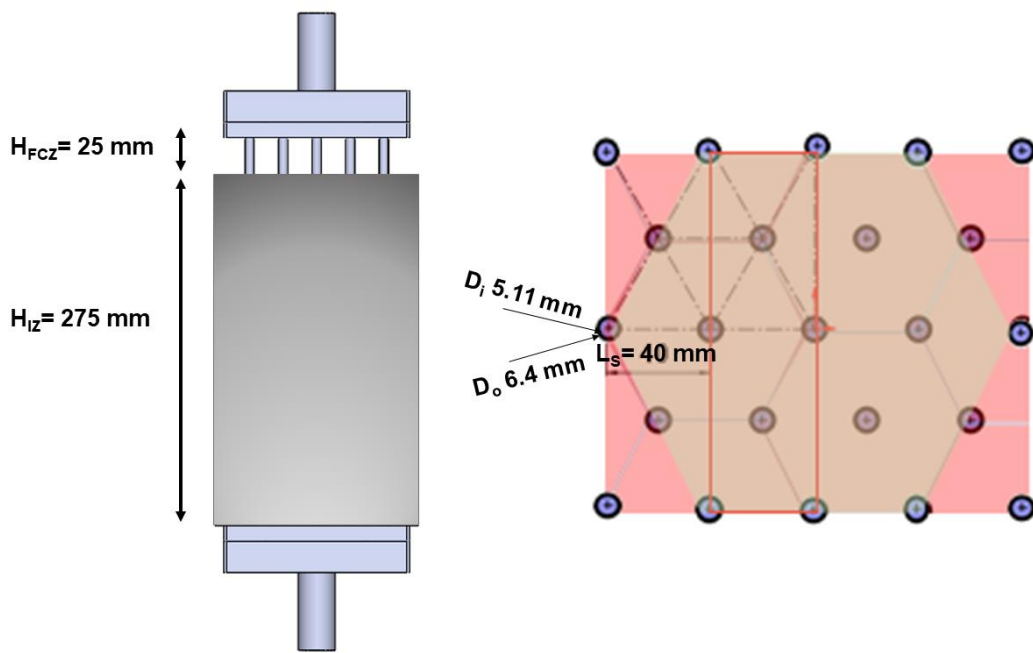


Figure S4. Geometry, boundary conditions and mesh of the multi-tubular fixed bed reactor design. Specification reactor design: Number of reactive channels=23; Geometry configuration=hexagonal-shaped distribution; Reactive channel distance separation=40 mm; Free-reactive zone=25 mm; Insulation active zone=225 mm.

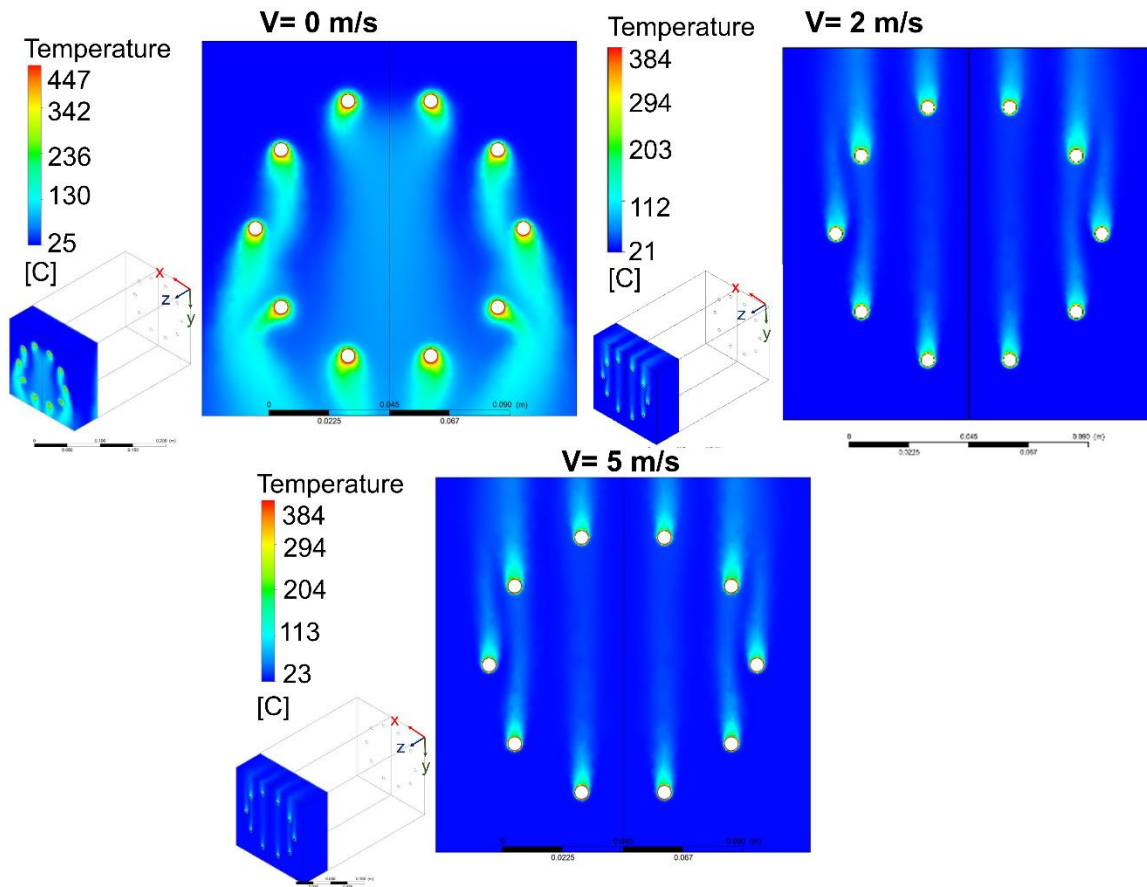


Figure S5. Influence of the air velocity on the temperature of the free-convective zone

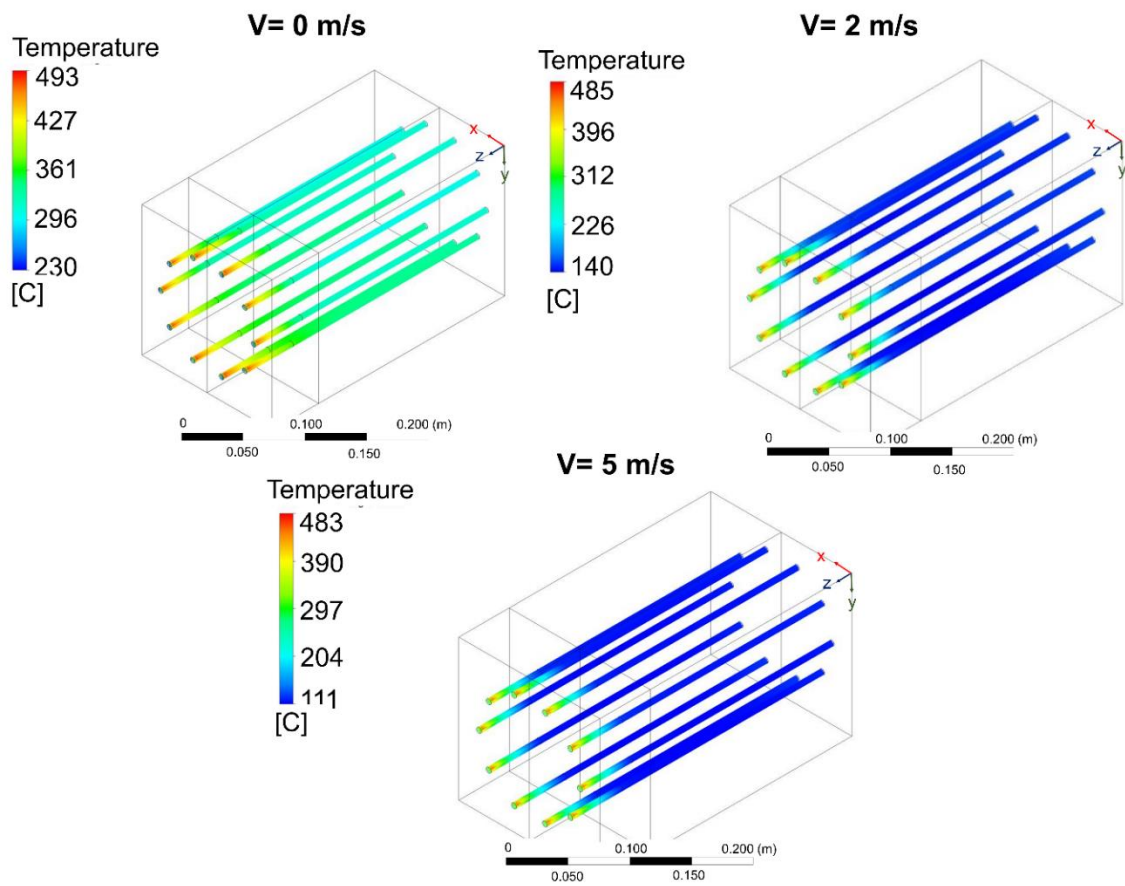


Figure S6. Influence of the air velocity on the temperature of the catalytic beds.

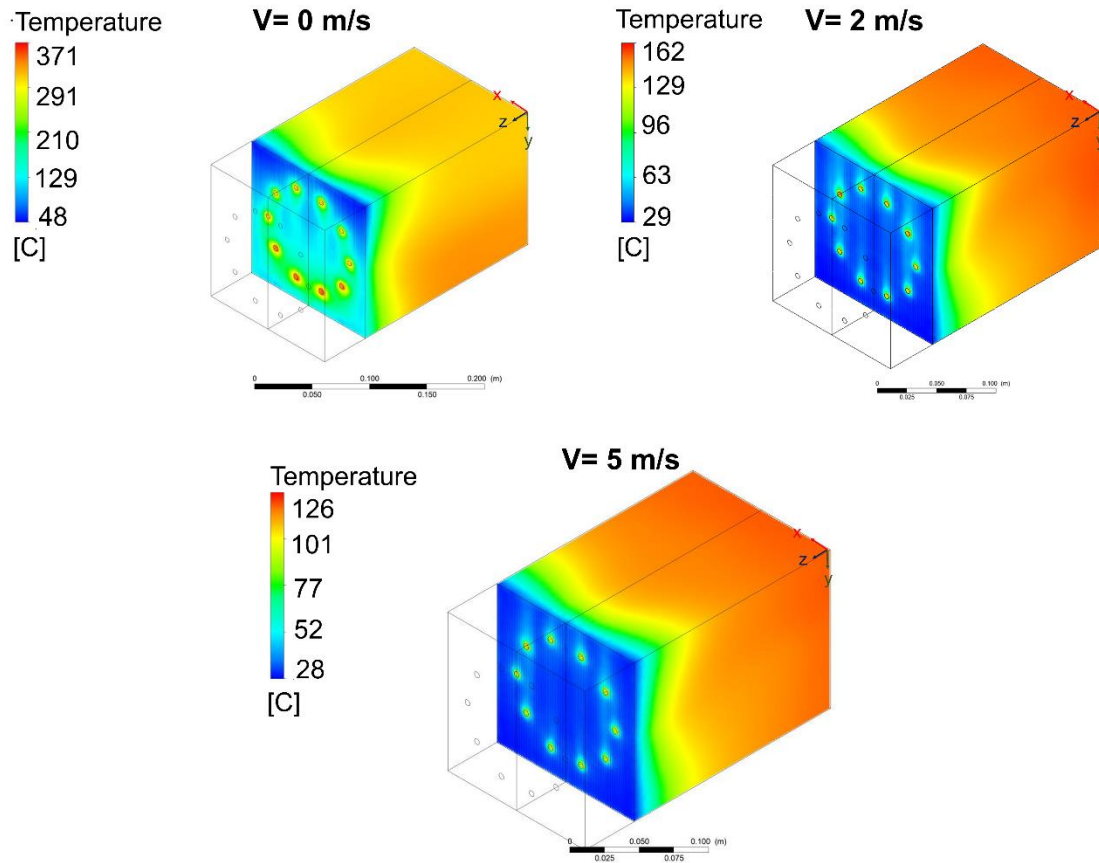


Figure S7. Influence of the air velocity on the temperature of the insulated zone

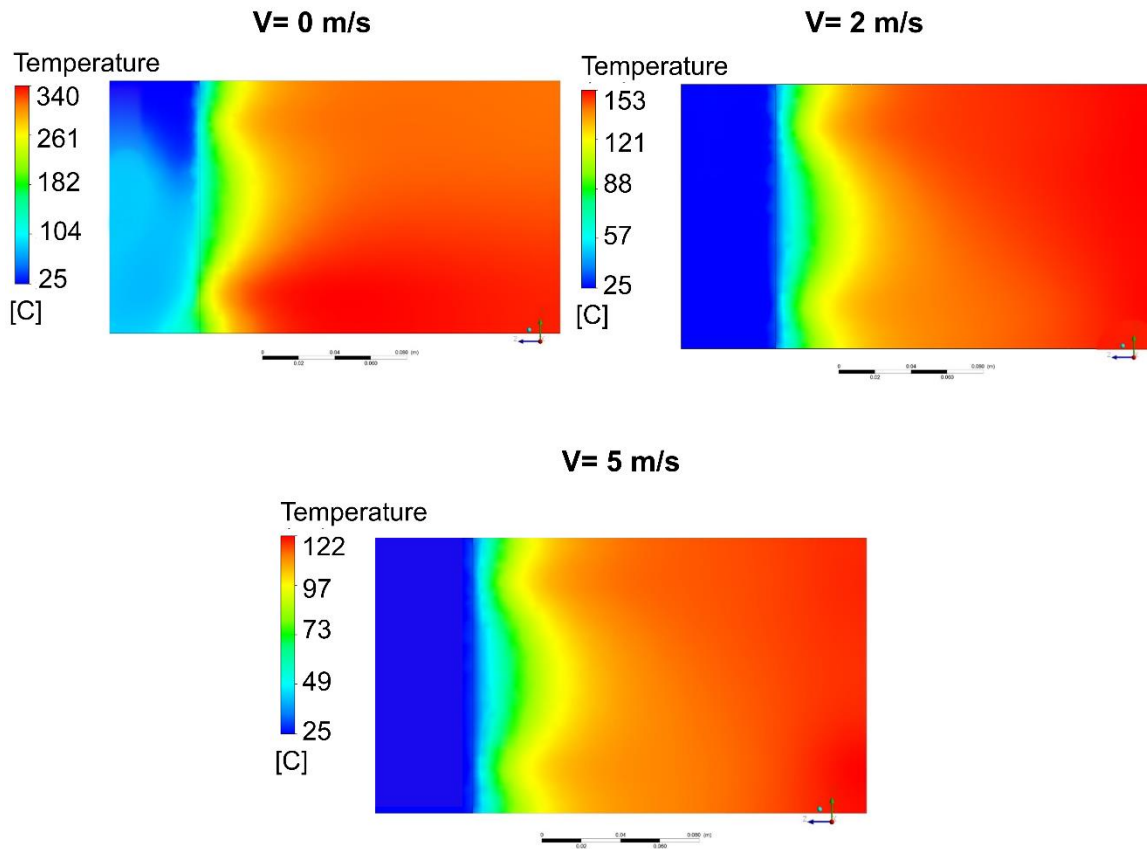


Figure S8. Influence of the air velocity on the temperature of the interior of the insulated zone

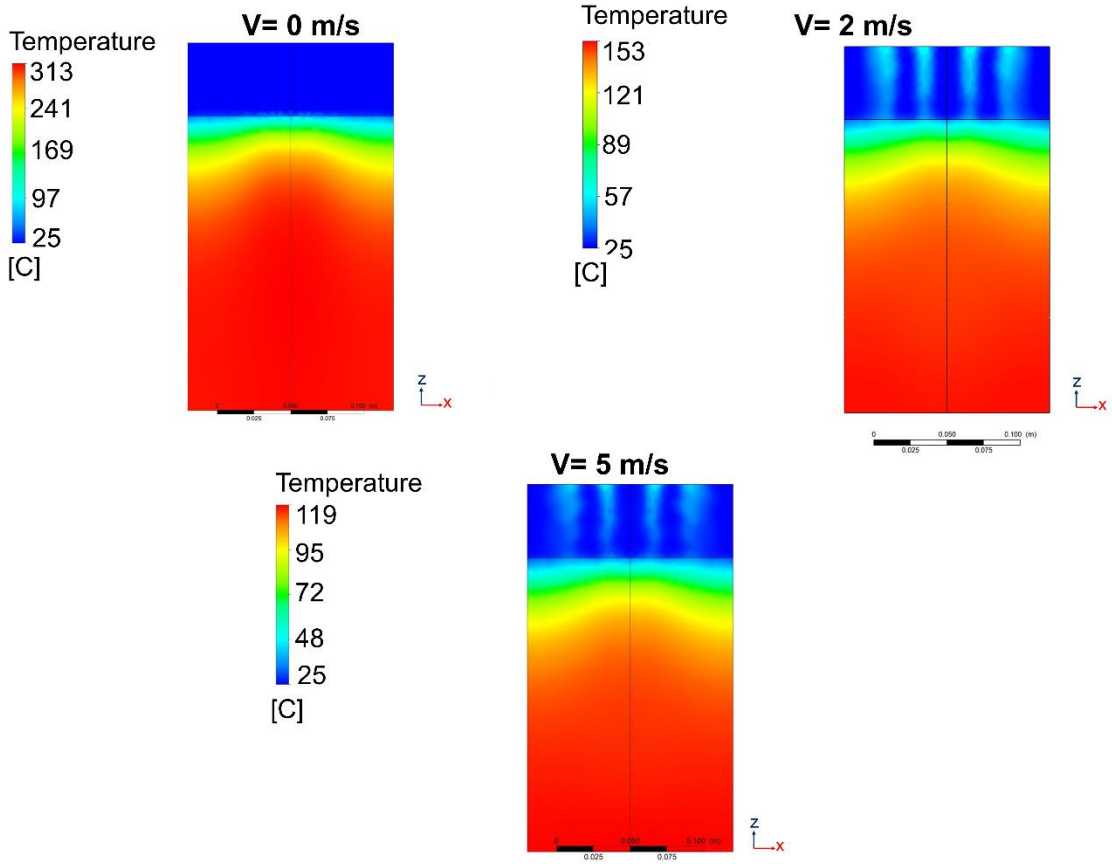


Figure S9. Influence of the air velocity on the temperature of the exterior of the insulated zone

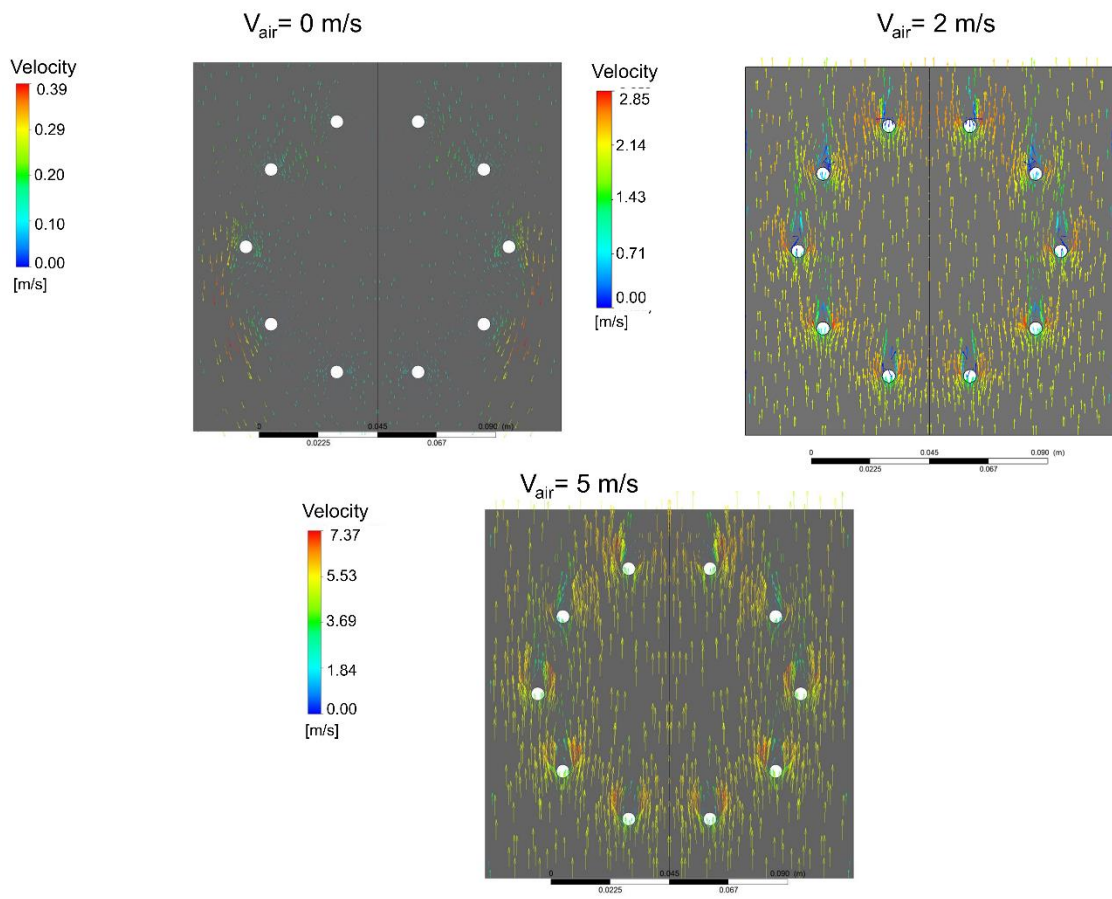


Figure S10. Velocity Profile of the multi-tubular fixed bed geometry configured with a total of 10 tubes under a hexagonal-shaped distribution.

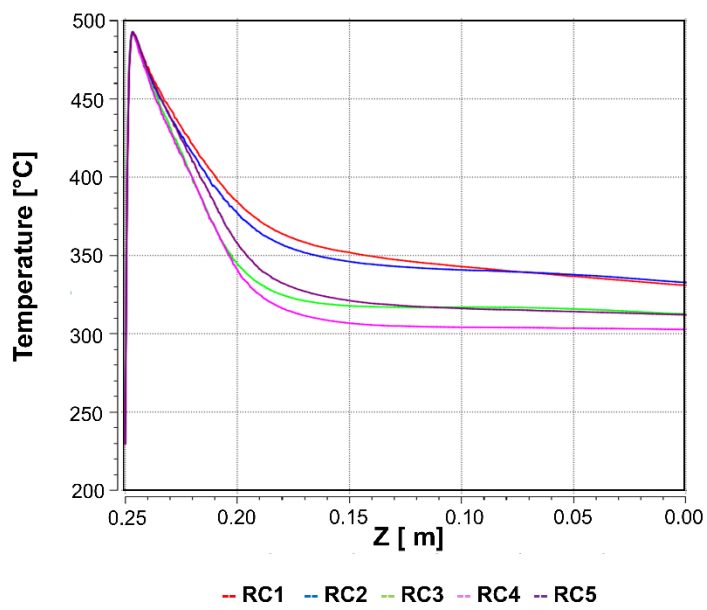


Figure S11. Temperature profiles of the catalytic beds at V_{air} of 0 m/s.

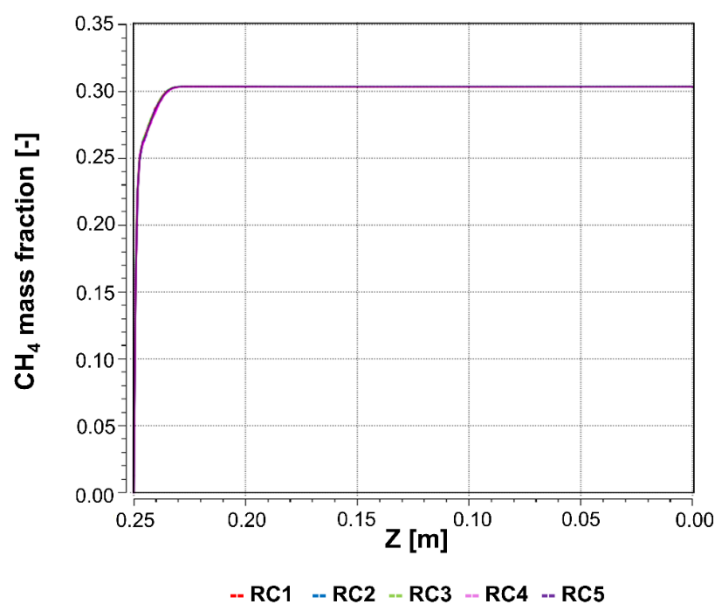


Figure S12. CH₄ mass fraction composition along of the catalytic beds at V_{air} of 5 m/s

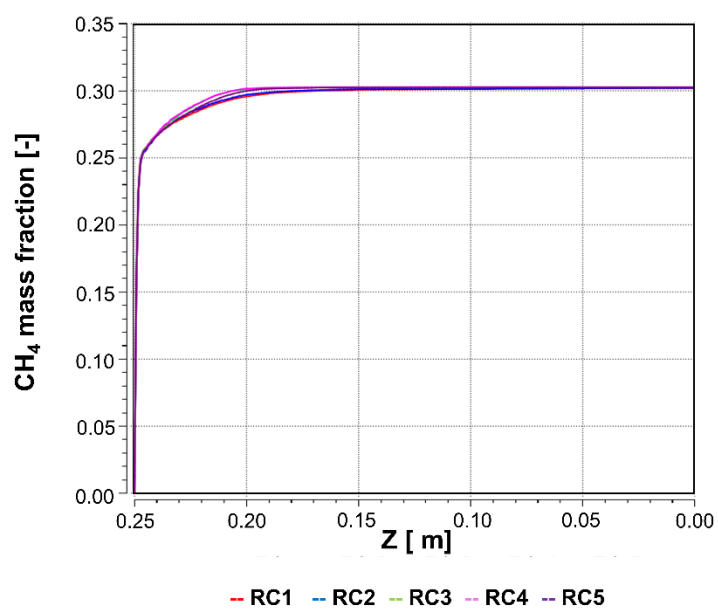


Figure S13. CH₄ mass fraction composition along of the catalytic beds at V_{air} of 0 m/s

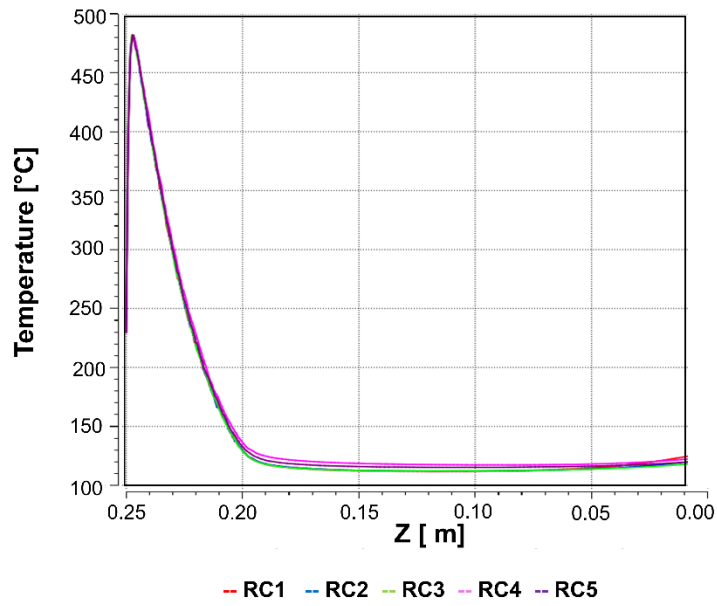


Figure S14. Temperature profiles of the catalytic beds at V_{air} of 5 m/s.

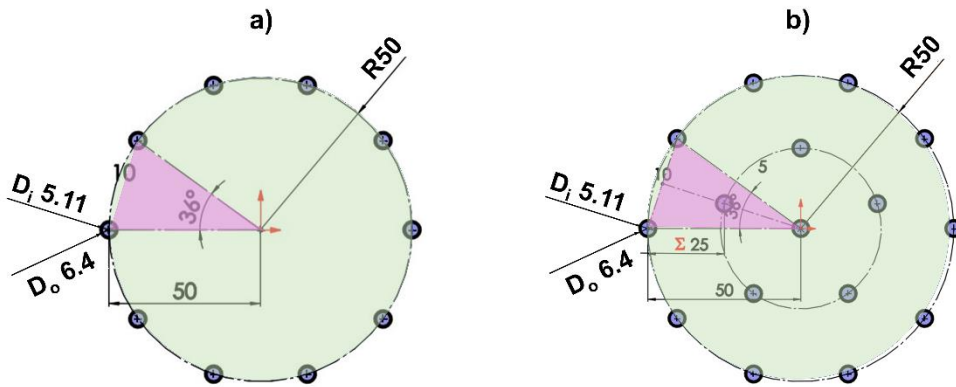


Figure S15. Multi-tubular fixed bed geometry configured with a circular-shaped distribution: a) 10 tubes and b) 16 tubes

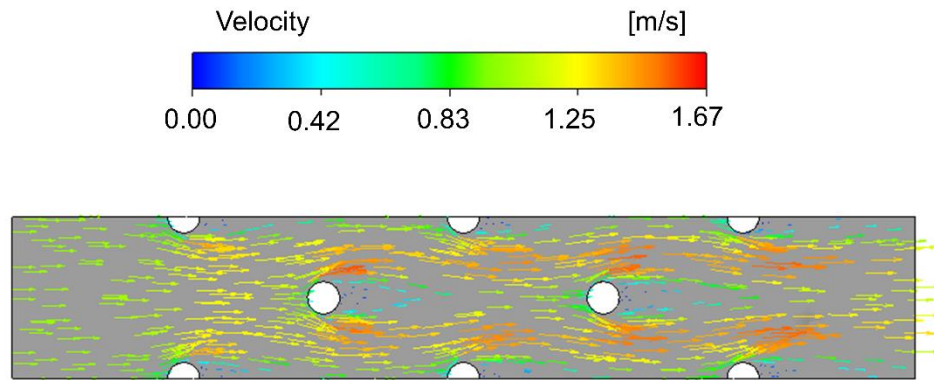


Figure S16. Velocity Profile of the multi-tubular fixed bed geometry configured with a total of 19 tubes under a hexagonal-shaped distribution.

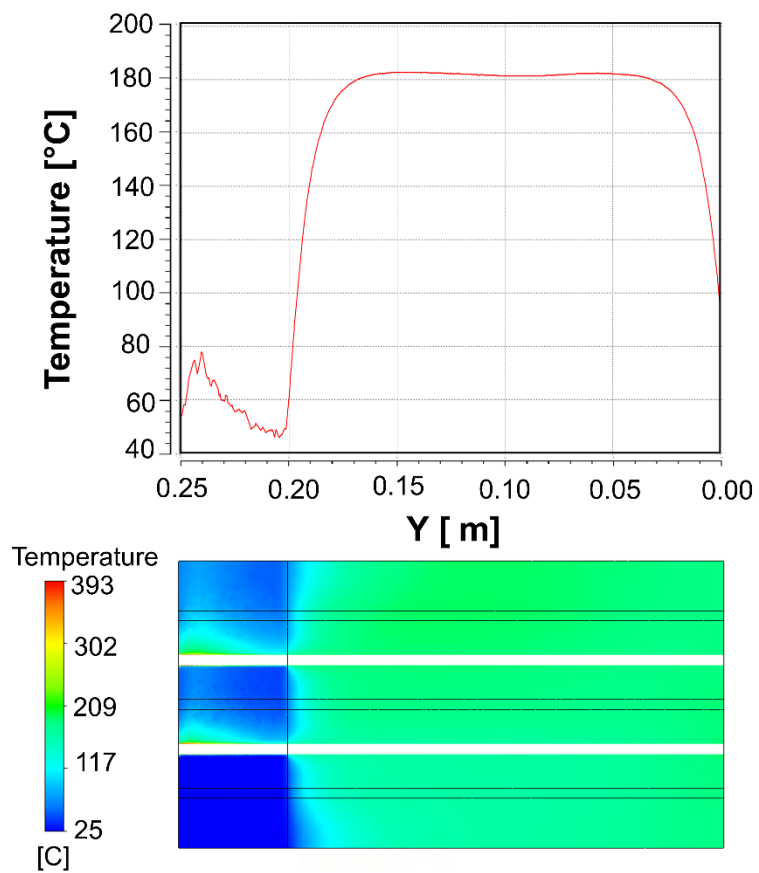


Figure S17. Temperature profile in an XY plane located in the interior of the insulation zone.

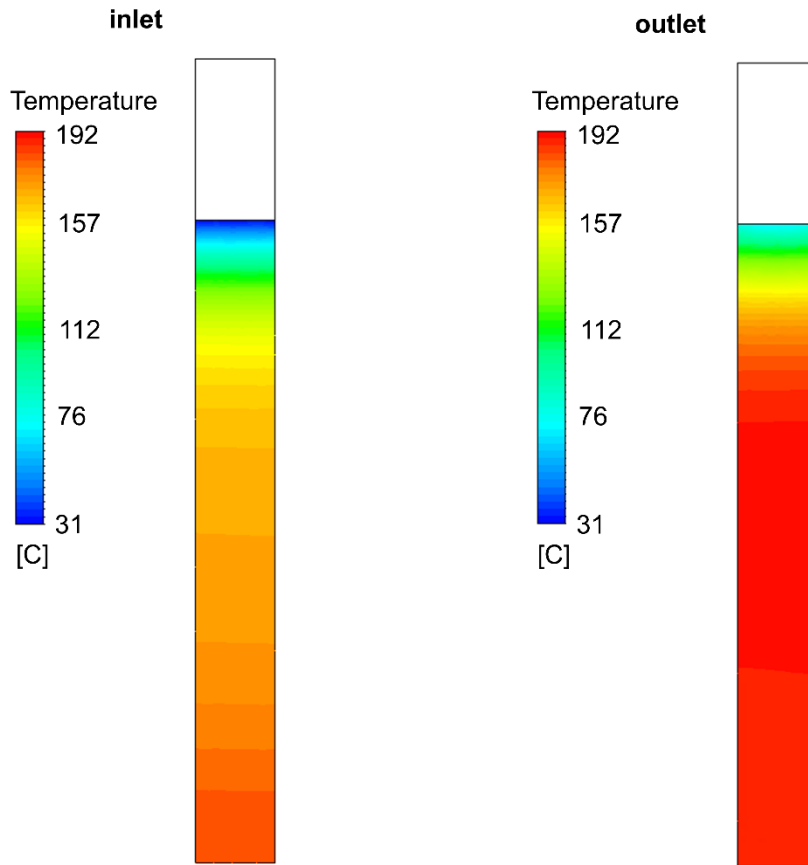


Figure S18. Temperature profile of the insulating material at inlet and outlet of the side of the air flow

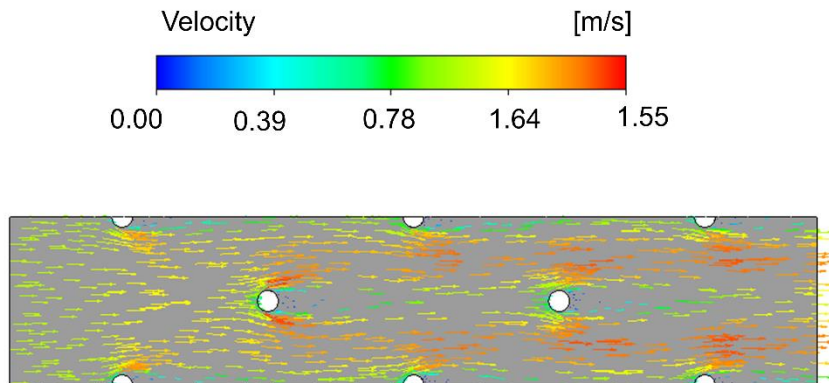


Figure S19. Velocity Profile of the multi-tubular fixed bed geometry configured with a total of 23 tubes under a hexagonal-shaped distribution.

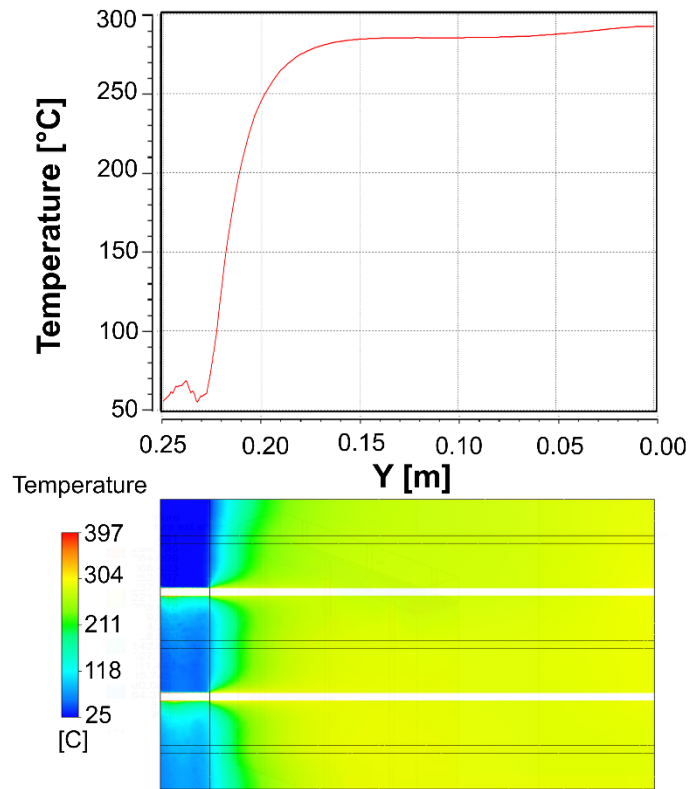


Figure S20. Temperature profile in an XY plane located in the interior of the insulation zone.

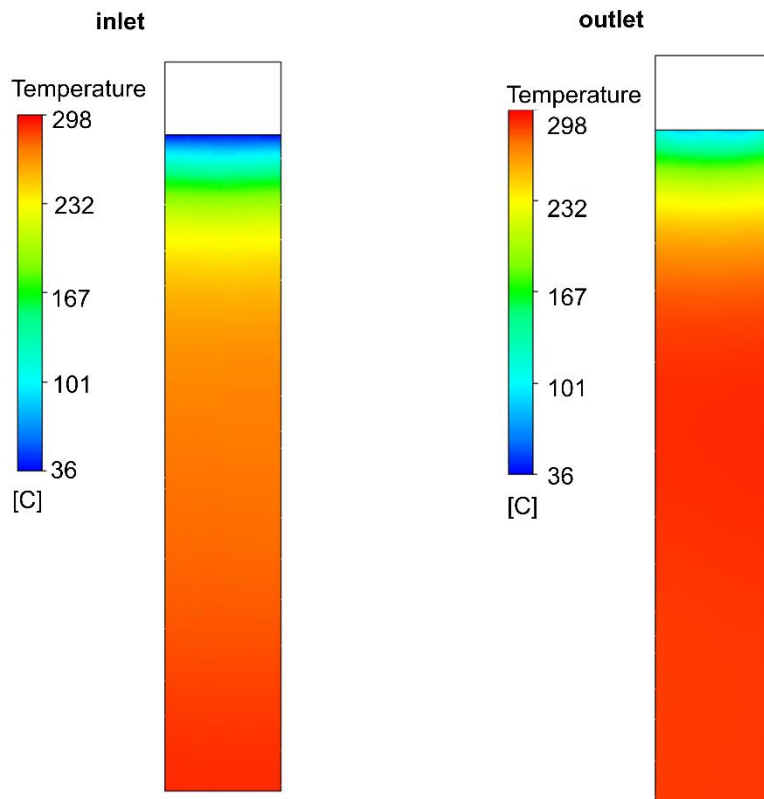


Figure S21. Temperature profile of the insulating material at inlet and outlet of the side of the air flow

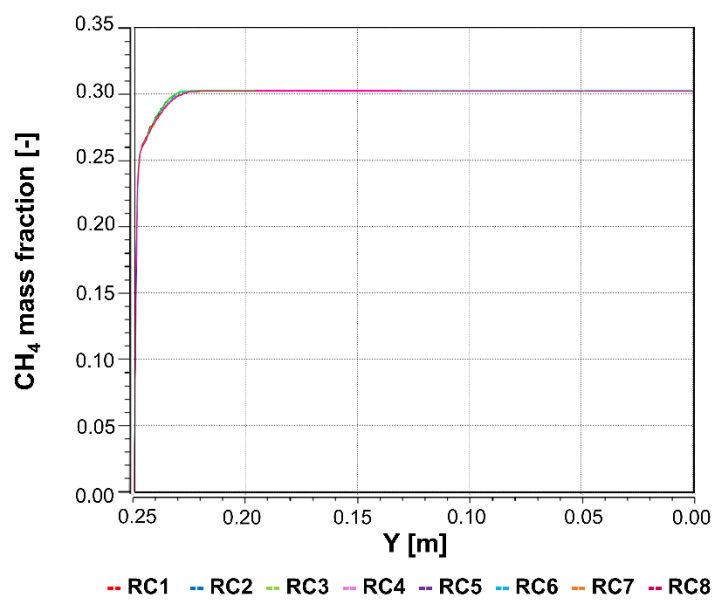


Figure S22. CH₄ mass fraction composition along of the catalytic beds at V_{air} of 1 m/s